Photometry of the Kuiper-Belt object 1999 TD_10 at different phase angles

P. Rousselot, Jean-Marc C. Petit, F. Poulet, P. Lacerda, J. Ortiz

A&A 407, 1139–1147 (2003)
DOI: 10.1051/0004-6361:20030850

Astronomy & Astrophysics

Photometry of the Kuiper-Belt object 1999 TD_{10} at different phase angles⋆,⋆⋆

P. Rousselot[1], J.-M. Petit[1], F. Poulet[2], P. Lacerda[3], and J. Ortiz[4]

[1] Besançon Observatory, BP 1615, 25010 Besançon Cedex, France
[2] Institut d'Astrophysique Spatiale, Bâtiment 121, Université Paris-Sud, 91405 Orsay Cedex, France
[3] Leiden Observatory, University of Leiden, Postbus 9513, 2300 RA Leiden, The Netherlands
[4] Instituto de Astrofísica de Andalucia, CSIC, Apt 3004, 18080 Granada, Spain

Received 8 January 2003 / Accepted 28 May 2003

Abstract. We present photometric observations of the Kuiper-Belt object 1999 TD_{10} at different phase angles and for three different broad band filters (*B*, *V* and *R*). This object was observed with the Danish 1.54-m telescope of ESO in Chile during six different observing nights corresponding to a phase angle of 0.30, 0.37, 0.92, 3.43, 3.48 and 3.66°. Extra observations were obtained in September 2002 with the VLT UT1/FORS1 combination to confirm that 1999 TD_{10} does not exhibit any cometary activity, and in October 2001 with the Sierra Nevada Observatory 1.50-m telescope in order to add relative magnitudes to improve the determination of the rotation period.
The observations are compatible with a single-peaked rotational lightcurve with a 7h41.5min ± 0.1 min period or a double-peaked lightcurve with a 15h22.9min ± 0.1 min period. If a single-peaked rotational lightcurve is assumed the amplitude is 0.51 ± 0.03, 0.49 ± 0.05 and 0.60 ± 0.09 mag for the *R*, *V* and *B* bands, respectively. We present the phase curve obtained when assuming that the lightcurve is single-peaked. This phase curve reveals clearly an increase of about 0.3 mag and of similar importance for the three bands when phase angle decreases from 3.7° to 0.3°. The phase curve reveals a linear increase of the brightness with the decreasing phase angle and, consequently, does not permit a modeling of the opposition surge. Neverthless the poor repartition of the observational data does not permit a firm conclusion concerning the presence or absence of an opposition surge on the phase angle range covered by our data. Complementary observations are needed.

Key words. solar system: general – Kuiper Belt – techniques: photometric

1. Introduction

The different populations of small bodies in the outer Solar System represent important clues to the formation and early evolution of that region. Given their relatively large number, the small bodies contain very valuable statistical information on the processes that created and sculpted these populations. Over the past decade the number of known objects has grown from almost nothing (a few giant planet irregular satellites and Centaurs) to a large number: 651 "classical" Trans-Neptunian Objects (TNOs), 127 Centaurs and Scattered Disk Objects (i.e. TNOs with a large eccentricity) and about 40 irregular satellites (as of January 2003).

Most of the observational studies of the TNOs are astrometric; a few studies of the luminosity distribution have also been done to constrain the formation and collisional evolution processes (Gladman et al. 2001; Trujillo et al. 2001). Some objects are bright enough ($R \leq 21$) to achieve spectrophotometric and/or low resolution spectroscopic observations which give a better knowledge of their physical and chemical properties (Barucci et al. 2000; Brown et al. 2000; Davies et al. 2000; Hainaut & Delsanti 2002; Jewitt & Luu 1998, 2001; Trujillo & Brown 2002).

Another method of analysis of the physical properties of planetary surfaces consists in studying how the reflected light varies with the phase angle, α. This approach has already been applied to many solid planetary surfaces. Regarding the Kuiper-Belt Objects (KBOs) and Centaurs, such a study represents a real challenge because of the low expected signal-to-noise of the observations even with large telescopes due to the faintness of these objects. Moreover, their large heliocentric distance limits the phase angles to a few degrees. So far, only a few preliminary results were obtained (Mc Bride et al. 1999; Bauer et al. 2002; Sheppard & Jewitt 2002;

Send offprint requests to: P. Rousselot,
e-mail: philippe@obs-besancon.fr

⋆ Tables 3, 4 and 5 are also available in electronic form at the CDS via anonymous ftp to cdsarc.u-strasbg.fr (130.79.128.5) or via http://cdsweb.u-strasbg.fr/cgi-bin/qcat?J/A+A/407/1139

⋆⋆ Based on observations obtained at the La Silla and the Very Large Telescope VLT observatories of the European Southern Observatory ESO in Chile.

Table 1. Orbital characteristics of 1999 TD_{10}.

a (AU)	e	q (AU)	Q (AU)	i
96.8	0.87	12.3	181.4	5.9°

Shaefer & Rabinowitz 2002). These results are sparse in terms of phase angle coverage, and are obtained in the *R*-band only.

In spite of the narrow range of phase angles, one can expect to detect the opposition surge, that is, a non-linear increase in surface brightness that occurs as the phase angle decreases to zero. Two causes to give rise to the opposition effect are usually considered: (1) shadow-hiding and (2) interference-enhancement, often called coherent-backscatter. Some general regolith properties-dependent characteristics of each mechanism are understood, and some papers are devoted to a discussion on the relative contribution of both mechanisms (Drossart 1993; Helfenstein et al. 1997, 1998; Hapke et al. 1998; Nelson et al. 2000; Belskaya & Shevchenko 2000; Shkuratov & Helfenstein 2001; Poulet et al. 2002). One can check for the effect of coherent backscatter and/or shadow hiding by studying the influence of wavelength of incident light on the opposition brigthening.

The goal of this paper is to present the results of a photometric study in different wavelength bands on one of the brightest and relatively red KBO classified as a Scattered Disk Object; 1999 TD_{10}. In the next section, the observations used here are described. Section 3 consists of derivation of the light and phase curves, and in Sect. 4, some discussion and interpretation of the rotational lightcurve and phase curve are presented.

1999 TD_{10} is a scattered disk object (Table 1) discovered on October 3, 1999 by Spacewatch. This object is one of the brightest KBO and, because of its large eccentricity, currently one of the closest from the Sun. Among all the scattered disk objects this one is rather unusual, since it has an orbit approaching that of comets and as well as Centaurs. It has already been observed by different observers in order to derive its color indices and magnitude (Delsanti et al. 2001; Lederer et al. 2002), its lightcurve (Choi et al. 2002; Consolmagno et al. 2000; Ortiz & Gutiérrez 2002) or its infrared spectrum (Brown 2000).

2. Observations and data reduction

The observations were performed at the Danish 1.54-m telescope of the European Southern Observatory in Chile. A total of 5 nights worth of data have been acquired during these observations. The data obtained during these nights cover the *R*, *V* and *B* bands, with images obtained regularly. Three more images were obtained, in the *R* band only, on October 1, 2001. Table 2 gives the details of the observing circumstances.

The observations were performed with the Danish Faint Object Spectrograph and Camera (DFOSC), a focal reducer instrument, equipped with a backside illuminated CCD chip 2048×4096 15 μm pixels. As the optics of DFOSC cannot utilise the whole area of the CCD, the readout area was only 2148×2102 pixels, which includes 50 pixel pre- and post-overscan regions in the *X*-direction and 22 masked pixels in the *Y*-direction. The CCD pixel scale was 0″.39/pix and the field of view $13.7' \times 13.7'$. Exposures were taken using Bessel *BVR* filters with typical sequences like RVRB.

Table 2. Observing circumstances (R: Heliocentric distance (AU); Δ: Geocentric distance (AU); α: phase angle).

UT Date	R	Δ	α
2001 Oct. 1	12.70	11.72	0.92°
2001 Oct. 8	12.71	11.71	0.37°
2001 Oct. 9	12.71	11.71	0.30°
2001 Nov. 30	12.77	12.13	3.43°
2001 Dec. 1	12.77	12.14	3.48°
2001 Dec. 5	12.78	12.20	3.66°

The seeing ranged from about 1.0 arcsec to 1.5 arcsec and the exposure time was 180 s during the October run and 360 s during the November-December run. With an apparent motion of 7.9″/hr and 2.4 to 3.3″/hr respectively during the October and November-December runs the trailing motion was always small compared to the seeing and so can be neglected as a source of error in the photometry. All the observing nights were photometric nights. During each of them two different fields of standard stars were regularly observed at different airmasses.

The images were bias-subtracted by using an averaged bias image and the overscan region. They were flat-fielded by using the median of a set of dithered images of the twilight sky. The photometric reduction was performed with the IRAF package by using the fields of standard stars, their brightness being measured by aperture photometry with a 10-pixel radius (3.9″). This photometric reduction took into account the three apparent magnitudes (*B*, *V* and *R*) measured at different airmasses in order to compute the transformation coefficients (zero point, extinction coefficient and color term).

Some other observations were carried out at the Sierra Nevada Observatory 1.5-m telescope during October 8, 9, 10, 2001 as part of a program whose first results are given in Ortiz et al. (2003). Briefly, we will mention that the images were taken using a fast readout 1024×1024 CCD with a field of view of 7×7 arcmin. The observations consisted in sequences of 100 s integrations with no filter. The typical seeing during the observations ranged from 1.1 arcsec to 2.5 arcsec, with median around 1.5 arcsec. The data reduction consisted in the typical bias subtraction and flatfield correction. The synthetic aperture photometry was carried out by using daophot routines. Seven field stars were used as references and the aperture diameter ranged from 2.4 to 4.0 arcsec. Details of the observing method and data reduction are given in Ortiz et al. (2003). Since this last set of observations gives only relative magnitude, it has been used only to improve the rotational lightcurve, and not the phase curve (see below).

3. Analysis

3.1. Photometry

For each image of 1999 TD_{10} 10 different flux measurements were performed: 5 with a 2.5-pixel radius (the object itself and

4 stars) and 5 with a 10-pixel radius (the same object and the same stars). The flux used to compute the final magnitude was the flux measured with a 2.5-pixel aperture and corrected for a 10-pixel aperture by using the other measurements on the four bright stars. The bright stars were also used to check that no brightness variations were appearent during the night, and so, to check the photometric character of the night as well as the quality of the photometric reduction. It is worth mentionning that the moon was very bright during the nights of November 30th and December 1st, leading to a degraded S/N ratio, especially in the B band.

During the November-December run the same field of view as the one used in October for 1999 TD_{10} was reobserved. The magnitude of a few stars visible in this field was measured by using the photometric coefficients computed during the November-December run, allowing to check the absolute consistancy of the two photometric reduction processes.

The three additional images obtained on October 1, 2001, with the R filter only, were processed by using the same flat-field and bias frames as the one obtained for October 8 and 9. The photometric coefficients used were also the same, because of lack of data with B and V filters. The consistancy of this data processing was checked on the standard stars images and confirmed the accuracy of this method (the R magnitudes computed by this method were found equal to better than 0.02 mag to the one given for these standards).

Tables 3, 4 and 5 present all the reduced magnitudes used for this work, respectively for filters R, V and B. Figure 1 graphically presents the same data.

Figure 2 presents a comparison of the radial profile obtained for 1999 TD_{10} with a comparison star. These two profiles have been computed using observational data obtained with the Very Large Telescope (VLT) in Chile, on September 4, 2002. Four different images obtained with this 8.2-m telescope, equipped with a focal reducer and low dispersion spectrograph called FORS 1, were co-added. The total integration time is 360 s, with a seeing of about 1 arcsec.

The examination of Fig. 2 reveals no sign of cometary activity, despite the claim by Choi et al. (2002). These authors used a 1-m telescope with a total integration time of 8400 s, i.e. a total collected flux about one third that collected in our VLT observations and presented in Fig. 2. Our conclusion is that we see no reason to attribute any change in the brightness of 1999 TD_{10} to a cometary activity.

3.2. Lightcurve

We derived the lightcurve from the data mentioned above by adding two corrections to the data given in Tables 3, 4 and 5. First we corrected the changing heliocentric and geocentric distances, which leads to a reduced magnitude given for the heliocentric and geocentric distances of October 8, 2001. The following formula was used:

$$\Delta M = 5[\log(\Delta(\mathrm{AU})/11.718) + \log(R(\mathrm{AU})/12.714)]. \quad (1)$$

This correction is the same for all data in a given night, but varies from night to night. So this is not important for the lightcurve per se, but rather for the phase curve. Ortiz et al. (2003) data are used only to calibrate the lightcurve, but they are not used for the phase curve because they were acquired without filter. Hence the magnitude correction is not applied to Ortiz et al. data.

Second we corrected the Modified Julian Date of the magnitudes in order to account for the light-time variations due to the changing geocentric distances. Once again the data obtained on October 8, 2001, were used as a reference (Δ = 11.718 AU). This correction was applied to all data, including Ortiz et al.

Following Harris et al. (1989), we modelled the light variation of 1999 TD_{10} as a Fourier expansion plus a phase effect:

$$H(\alpha,t) = \bar{H}(\alpha) + \sum_{l=1}^{m}\left[A_l \sin\frac{2\Pi l}{P}(t-t_0) + B_l \cos\frac{2\Pi l}{P}(t-t_0)\right] \quad (2)$$

where $H(\alpha,t)$ is the computed magnitude at given phase angle and time t, $\bar{H}(\alpha)$ is the mean magnitude at phase angle α, A_l and B_l are Fourier coefficients, P is the rotation period, t_0 is a zero point time and m is the order of expansion.

The Fourier expansion in the above formula gives the *rotational lightcurve* of the object. This informs us on the rotation state and shape of the body. The first term in Eq. (2) represents the phase effect, that is, the variation of flux due to changing illumination and viewing geometries. As described in Sect. 4, it contains information about the physical properties of the surface.

In absence of any indication of the probability distribution of the parameters in the model, we chose to fit them to the data using a χ^2 fitting technic (Press et al. 1992). One can see that Eq. (2) does not depend linearly on all parameters. In order to make processing simpler, and avoid having the non-linear methods wandering in non desirable parts of the parameter space, we divided the problem into 2 simpler ones. We first merged the R filters data with Ortiz et al. filter free data. Using these, we estimated the rotation period. Still using these data, we then fixed the period and the order of expansion in Eq. (2) and searched for the best fitting parameters. For this best fit set of parameters, we computed the bias-corrected χ^2, that is, χ^2 divided by the number of degree of freedom $f = n-2m-p-1$ (n number of data, p number of nights of data and 1 for the period). We then varied the period and the order of expansion. The period and the maximum order of expansion was finally selected by finding the lowest bias-corrected χ^2. We then came back to each individual filtered data set. We used the same previously determined period, and the actual order of expansion was taken to be smaller than or equal to the maximum order of expansion as defined before while minimizing the bias-corrected χ^2 for that data set.

The first step was to determine a good approximation of the rotation period. From the first second and third nights of observations in R, we can infer that the period is close to 24 hours divided by an integer number (see Fig. 1). In the same time, one can clearly see that it is longer than 6.5 hours, contrary to the value of 5.8 hours proposed by Consolmagno et al. (2000).

Table 3. Photometric data of 1999 TD_{10} used for this work, for the *R* filter. MJD represents the Modified Julian Date – 52000 and is given for mid-frames.

UT Date	MJD	Mag.	UT Date	MJD	Mag.
2001 Oct. 1	183.2936	19.215 ±0.100	2001 Oct. 9	191.2495	19.123 ±0.034
2001 Oct. 1	183.3019	19.302 ±0.100	2001 Oct. 9	191.2569	19.122 ±0.020
2001 Oct. 1	183.3112	19.315 ±0.100	2001 Oct. 9	191.2635	19.091 ±0.018
2001 Oct. 8	190.0989	19.499 ±0.032	2001 Oct. 9	191.2758	19.120 ±0.019
2001 Oct. 8	190.1059	19.560 ±0.032	2001 Oct. 9	191.2826	19.120 ±0.015
2001 Oct. 8	190.1133	19.540 ±0.025	2001 Oct. 9	191.2898	19.155 ±0.012
2001 Oct. 8	190.1425	19.580 ±0.025	2001 Oct. 9	191.2965	19.160 ±0.012
2001 Oct. 8	190.1492	19.595 ±0.026	2001 Oct. 9	191.3038	19.189 ±0.015
2001 Oct. 8	190.1598	19.566 ±0.024	2001 Oct. 9	191.3105	19.218 ±0.012
2001 Oct. 8	190.1675	19.547 ±0.025	2001 Oct. 9	191.3227	19.198 ±0.026
2001 Oct. 8	190.1753	19.493 ±0.028	2001 Oct. 9	191.3294	19.233 ±0.019
2001 Oct. 8	190.1820	19.479 ±0.032	2001 Oct. 9	191.3367	19.332 ±0.020
2001 Oct. 8	190.1963	19.439 ±0.030	2001 Oct. 9	191.3434	19.338 ±0.020
2001 Oct. 8	190.2033	19.378 ±0.028	2001 Nov. 30	243.0373	19.896 ±0.036
2001 Oct. 8	190.2105	19.327 ±0.034	2001 Nov. 30	243.0486	19.887 ±0.059
2001 Oct. 8	190.2172	19.312 ±0.029	2001 Nov. 30	243.0710	19.829 ±0.045
2001 Oct. 8	190.2246	19.299 ±0.035	2001 Nov. 30	243.0827	19.824 ±0.052
2001 Oct. 8	190.2313	19.240 ±0.031	2001 Nov. 30	243.0934	19.774 ±0.044
2001 Oct. 8	190.2388	19.215 ±0.027	2001 Nov. 30	243.1115	19.736 ±0.061
2001 Oct. 8	190.2455	19.195 ±0.029	2001 Nov. 30	243.1226	19.684 ±0.048
2001 Oct. 8	190.2617	19.192 ±0.039	2001 Nov. 30	243.1395	19.708 ±0.055
2001 Oct. 8	190.2686	19.156 ±0.050	2001 Nov. 30	243.1506	19.554 ±0.058
2001 Oct. 8	190.2758	19.132 ±0.047	2001 Nov. 30	243.1615	19.648 ±0.043
2001 Oct. 8	190.2825	19.086 ±0.051	2001 Nov. 30	243.1723	19.584 ±0.047
2001 Oct. 8	190.2898	19.119 ±0.048	2001 Nov. 30	243.1916	19.501 ±0.049
2001 Oct. 8	190.2965	19.097 ±0.051	2001 Nov. 30	243.2031	19.543 ±0.066
2001 Oct. 8	190.3045	19.090 ±0.043	2001 Dec. 1	244.0204	20.062 ±0.075
2001 Oct. 8	190.3111	19.083 ±0.041	2001 Dec. 1	244.0319	20.009 ±0.071
2001 Oct. 8	190.3243	19.128 ±0.052	2001 Dec. 1	244.0429	19.864 ±0.044
2001 Oct. 8	190.3313	19.111 ±0.047	2001 Dec. 1	244.0537	19.760 ±0.035
2001 Oct. 8	190.3386	19.168 ±0.047	2001 Dec. 1	244.0654	19.795 ±0.038
2001 Oct. 9	191.0823	19.530 ±0.032	2001 Dec. 1	244.0762	19.806 ±0.033
2001 Oct. 9	191.0893	19.574 ±0.017	2001 Dec. 1	244.0872	19.709 ±0.038
2001 Oct. 9	191.0966	19.577 ±0.035	2001 Dec. 1	244.0980	19.673 ±0.032
2001 Oct. 9	191.1033	19.633 ±0.034	2001 Dec. 1	244.1165	19.686 ±0.045
2001 Oct. 9	191.1105	19.619 ±0.026	2001 Dec. 1	244.1276	19.614 ±0.042
2001 Oct. 9	191.1172	19.633 ±0.020	2001 Dec. 1	244.1386	19.577 ±0.035
2001 Oct. 9	191.1245	19.580 ±0.019	2001 Dec. 1	244.1494	19.594 ±0.044
2001 Oct. 9	191.1312	19.529 ±0.023	2001 Dec. 1	244.1668	19.577 ±0.033
2001 Oct. 9	191.1385	19.513 ±0.021	2001 Dec. 1	244.1776	19.611 ±0.046
2001 Oct. 9	191.1452	19.489 ±0.025	2001 Dec. 5	248.0304	19.691 ±0.044
2001 Oct. 9	191.1525	19.435 ±0.030	2001 Dec. 5	248.0416	19.755 ±0.048
2001 Oct. 9	191.1592	19.420 ±0.035	2001 Dec. 5	248.0531	19.747 ±0.036
2001 Oct. 9	191.1664	19.414 ±0.027	2001 Dec. 5	248.0639	19.851 ±0.040
2001 Oct. 9	191.1731	19.355 ±0.021	2001 Dec. 5	248.0749	19.867 ±0.058
2001 Oct. 9	191.1804	19.300 ±0.023	2001 Dec. 5	248.0857	19.942 ±0.059
2001 Oct. 9	191.1871	19.273 ±0.021	2001 Dec. 5	248.0969	19.913 ±0.090
2001 Oct. 9	191.2045	19.219 ±0.029	2001 Dec. 5	248.1077	20.079 ±0.091
2001 Oct. 9	191.2112	19.211 ±0.023	2001 Dec. 5	248.1261	20.055 ±0.053
2001 Oct. 9	191.2190	19.170 ±0.028	2001 Dec. 5	248.1369	20.120 ±0.068
2001 Oct. 9	191.2257	19.151 ±0.016	2001 Dec. 5	248.1537	20.131 ±0.073
2001 Oct. 9	191.2427	19.132 ±0.021	2001 Dec. 5	248.1645	20.103 ±0.093

If the curve is assumed to be single-peaked, the period is slightly shorter than 8 hours. To obtain a more precise value, we had to resort to spectral analysis of the combined *R* filter and Ortiz et al. data. Since our data is unevenly sampled and sparse, we computed the Lomb *normalized periodogram* (Press et al. 1992). We investigated frequencies in the largest possible range, from the lowest one, corresponding to the inverse of the total time span of observations, to a frequency larger than

Table 4. Photometric data of 1999 TD_{10} used for this work, for the *V* filter. MJD represents the Modified Julian Date – 52 000 and is given for mid-frames.

UT Date	MJD	Mag.
2001 Oct. 8	190.1026	20.045 ±0.039
2001 Oct. 8	190.1166	20.042 ±0.048
2001 Oct. 8	190.1459	20.037 ±0.034
2001 Oct. 8	190.1641	19.988 ±0.053
2001 Oct. 8	190.1787	19.984 ±0.063
2001 Oct. 8	190.1999	19.868 ±0.061
2001 Oct. 8	190.2138	19.818 ±0.049
2001 Oct. 8	190.2279	19.795 ±0.069
2001 Oct. 8	190.2421	19.688 ±0.048
2001 Oct. 8	190.2652	19.594 ±0.060
2001 Oct. 8	190.2792	19.607 ±0.055
2001 Oct. 8	190.2931	19.542 ±0.059
2001 Oct. 8	190.3078	19.590 ±0.067
2001 Oct. 8	190.3280	19.576 ±0.080
2001 Oct. 9	191.0860	20.044 ±0.043
2001 Oct. 9	191.0999	20.080 ±0.046
2001 Oct. 9	191.1139	20.099 ±0.034
2001 Oct. 9	191.1279	20.057 ±0.038
2001 Oct. 9	191.1418	19.995 ±0.031
2001 Oct. 9	191.1558	19.950 ±0.040
2001 Oct. 9	191.1698	19.893 ±0.044
2001 Oct. 9	191.1837	19.799 ±0.032
2001 Oct. 9	191.2079	19.680 ±0.034
2001 Oct. 9	191.2223	19.672 ±0.025
2001 Oct. 9	191.2462	19.600 ±0.038
2001 Oct. 9	191.2602	19.625 ±0.034
2001 Oct. 9	191.2792	19.609 ±0.031
2001 Oct. 9	191.2932	19.675 ±0.044
2001 Oct. 9	191.3071	19.696 ±0.045
2001 Oct. 9	191.3261	19.729 ±0.037
2001 Oct. 9	191.3401	19.826 ±0.041
2001 Nov. 30	243.0432	20.631 ±0.087
2001 Nov. 30	243.0656	20.402 ±0.075
2001 Nov. 30	243.0881	20.347 ±0.080
2001 Nov. 30	243.1172	20.165 ±0.080
2001 Nov. 30	243.1452	20.031 ±0.070
2001 Nov. 30	243.1669	19.793 ±0.164
2001 Nov. 30	243.1977	19.984 ±0.109
2001 Dec. 1	244.0708	20.126 ±0.057
2001 Dec. 1	244.0926	20.190 ±0.092
2001 Dec. 1	244.1222	20.112 ±0.093
2001 Dec. 1	244.1440	20.072 ±0.056
2001 Dec. 1	244.1722	20.148 ±0.102
2001 Dec. 5	248.0362	20.134 ±0.040
2001 Dec. 5	248.0585	20.181 ±0.052
2001 Dec. 5	248.0803	20.290 ±0.048
2001 Dec. 5	248.1023	20.427 ±0.070
2001 Dec. 5	248.1315	20.572 ±0.091
2001 Dec. 5	248.1591	20.580 ±0.095

Table 5. Photometry of 1999 TD_{10} used for this work, for the *B* filter. MJD represents the Modified Julian Date – 52 000 and is given for mid-frames.

UT Date	MJD	Mag.
2001 Oct. 8	190.1095	20.733 ±0.075
2001 Oct. 8	190.1375	20.835 ±0.048
2001 Oct. 8	190.1528	20.868 ±0.051
2001 Oct. 8	190.1711	20.780 ±0.055
2001 Oct. 8	190.1856	20.710 ±0.113
2001 Oct. 8	190.2069	20.585 ±0.081
2001 Oct. 8	190.2208	20.649 ±0.131
2001 Oct. 8	190.2349	20.416 ±0.086
2001 Oct. 8	190.2491	20.464 ±0.111
2001 Oct. 8	190.2722	20.371 ±0.094
2001 Oct. 8	190.2861	20.427 ±0.164
2001 Oct. 8	190.3001	20.288 ±0.136
2001 Oct. 8	190.3148	20.294 ±0.151
2001 Oct. 8	190.3349	20.389 ±0.120
2001 Oct. 9	191.0929	20.941 ±0.081
2001 Oct. 9	191.1069	20.838 ±0.080
2001 Oct. 9	191.1208	20.926 ±0.049
2001 Oct. 9	191.1348	20.835 ±0.041
2001 Oct. 9	191.1488	20.624 ±0.075
2001 Oct. 9	191.1628	20.585 ±0.065
2001 Oct. 9	191.1767	20.632 ±0.065
2001 Oct. 9	191.1907	20.555 ±0.056
2001 Oct. 9	191.2148	20.471 ±0.042
2001 Oct. 9	191.2293	20.381 ±0.080
2001 Oct. 9	191.2531	20.259 ±0.059
2001 Oct. 9	191.2651	20.377 ±0.056
2001 Oct. 9	191.2862	20.285 ±0.099
2001 Oct. 9	191.3001	20.465 ±0.075
2001 Oct. 9	191.3141	20.444 ±0.061
2001 Oct. 9	191.3330	20.495 ±0.097
2001 Oct. 9	191.3470	20.639 ±0.109
2001 Nov. 30	243.0541	21.441 ±0.287
2001 Nov. 30	243.0765	21.127 ±0.191
2001 Nov. 30	243.0989	20.980 ±0.218
2001 Nov. 30	243.1281	21.013 ±0.159
2001 Nov. 30	243.1560	20.896 ±0.205
2001 Dec. 1	244.0591	20.873 ±0.277
2001 Dec. 1	244.0817	21.056 ±0.213
2001 Dec. 1	244.1034	21.113 ±0.300
2001 Dec. 1	244.1331	20.019 ±0.350
2001 Dec. 1	244.1549	20.462 ±0.196
2001 Dec. 1	244.1831	20.899 ±0.363
2001 Dec. 5	248.0471	20.942 ±0.123
2001 Dec. 5	248.0694	21.039 ±0.068
2001 Dec. 5	248.0912	21.063 ±0.108
2001 Dec. 5	248.1131	21.153 ±0.107
2001 Dec. 5	248.1424	21.273 ±0.125
2001 Dec. 5	248.1700	21.374 ±0.286

the expected one, namely up to 8 rotations per day (period of 3 hours).

The periodogram shows strong maxima close to, but slightly larger than each integer number of rotations per days. The first four maxima correspond to periods of 20h45.5min, 11h02.5min, 7h41.3min and 5h47.6min. This last value corresponds to the period proposed by Consolmagno et al. (2000). However, looking at Fig. 1, one can easily determine the period to be close to the third maximum, i.e. close to 7h41.3min. We then fitted the data with periods from 7h29min to 7h49min with 0.1 min increments, and expansion orders from 1 to 20. From this study, we determined a period of

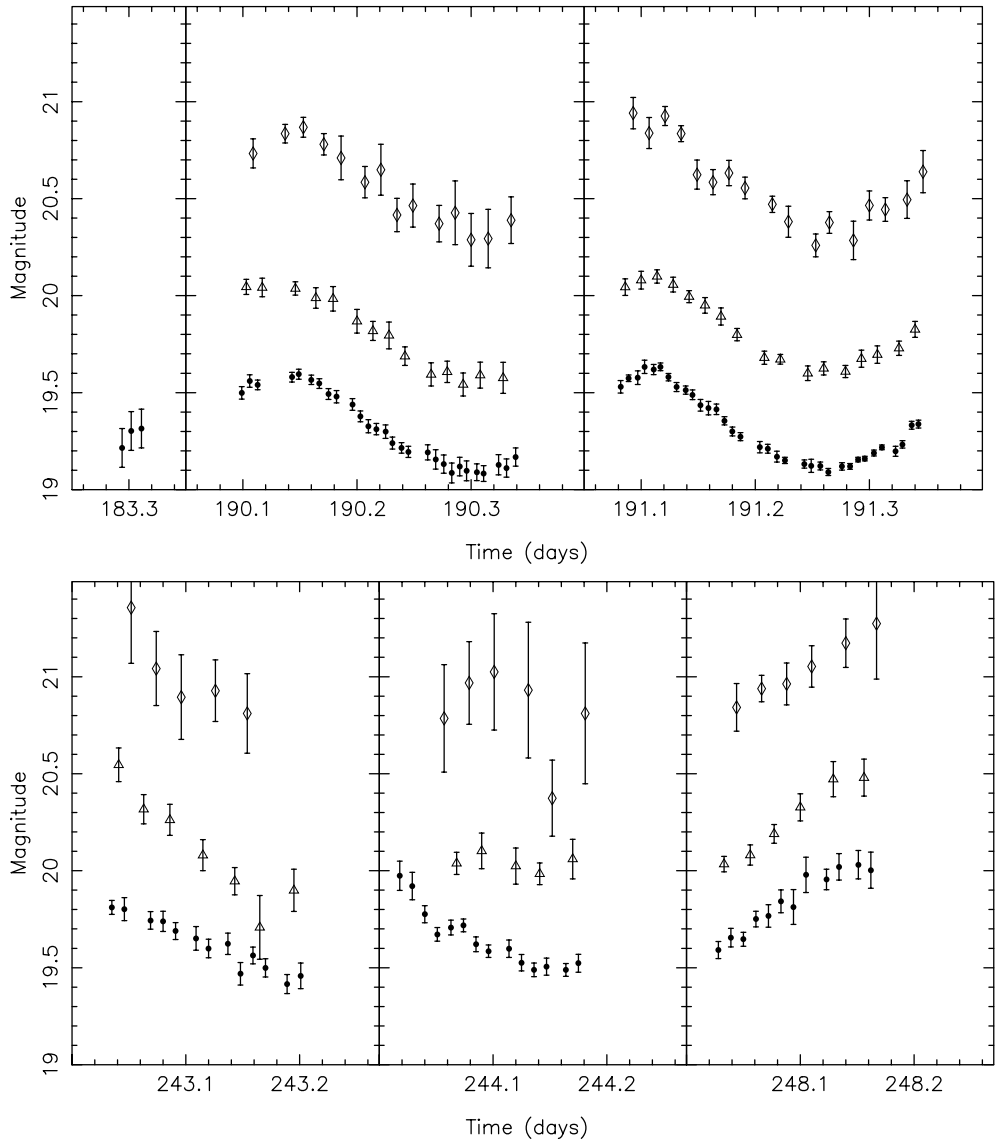

Fig. 1. Measured magnitudes in the 3 filters, *R* (filled circles), *V* (triangles) and *B* (diamonds) for the six different nights of observations available. The time is given in Modified Julian Date – 52 000.

7h41.5min ± 0.1min, and a maximum order of expansion of 8. We then fitted the individual filtered data sets with period 7h41.5min, and order of expansion 6 for *R* filter and 5 for both *B* and *V* filters. Figure 3a shows actual data, shifted in time according to this period, and shifted in magnitude according to the phase effect (see below). The computed magnitude (Eq. (2)), shifted accordingly, is superimposed on the plot.

We applied the same method to the other periods proposed by the Lomb normalized periodogram, and obtained a best fit bias corrected χ^2 three times larger than for period 7h41.5min. Hence we can conclude that these periods are artifacts due to the sampling periodicity.

Assuming that the lightcurve has a double peak shape (to be expected if we suppose the brightness variation to be due to an elongated shape of 1999 TD_{10}), the same method gives a period of 15h22.9min ± 0.1min, or twice the previous one, within the error bars. Figure 3b presents the same data as Fig. 3a, but for a double-peaked lightcurve. However the periodogram did not show any local maximum for that period. One can then suppose that this double peak shape is just a repetition of the single peak with period 7h41.5min.

3.3. Phase function

The phase curve was determined by specifying a function form for $\bar{H}(\alpha)$. Since we have only 5 nights of data (6 for *R* filter), and the phase angle α does not vary much during a given night, we modeled the phase curve with a stepwise function, with 5 (or 6) different values for both possible lightcurve (single-peaked or double-peaked). Therefore, the computed magnitude $H(\alpha, t)$ depends linearly on the Fourier coefficients and the $p = 5$ (or 6) values of $\bar{H}(\alpha)$. Hence the previous fitting provided us with 5 (or 6) values of $\bar{H}(\alpha)$ for each filter, which are presented in Fig. 4 as a function of phase angle α. Figure 4 presents the results obtained when assuming that the lightcurve is single-peaked. The results obtained when assuming that the

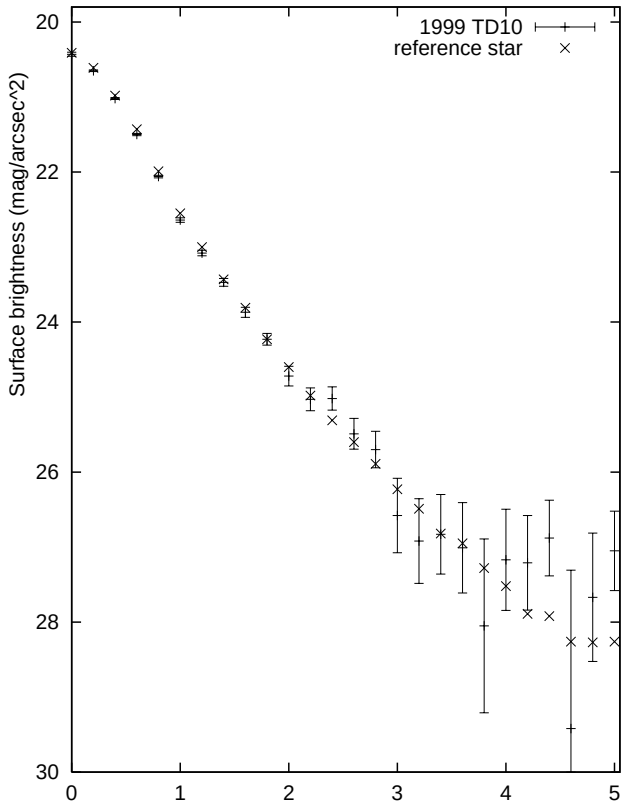

Fig. 2. Comparison of the radial profile of 1999 TD10 with a reference star obtained by co-adding four different images obtained with the VLT for a total integration time of 6 min.

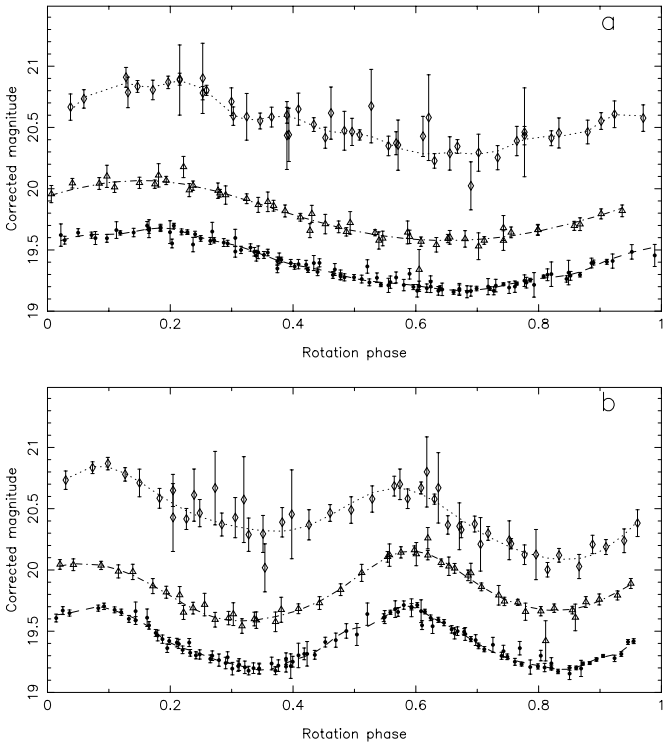

Fig. 3. Corrected magnitudes (dots with error bars) for *R* (filled circles), *V* (triangles) and *B* (diamonds) filters. The time axis has been folded to display a single-peaked lightcurve with a 7h41.5min period **a)** or a double-peaked lightcurve with a 15h22.9min period **b)**. The magnitudes have been shifted according to the phase effect (see Fig. 4) to all fit on the same curve. The lines are drawn with Eq. (2) and the best fit parameters for the given period and expansion orders given in the text.

lightcurve is double-peaked are, nevertheless, very similar and lead to the same conclusions.

The error bars on the parameters can in principle be estimated from the uncertainty of the data points and the computation of the best fit parameters (Press et al. 1992). However, this assumes that our estimate of the absolute error on the data is correct. In order to confirm those values, we also used a Monte Carlo method to determine the uncertainties on the parameters, as described in Press et al. (1992). From the best fit we already obtained, we estimated the variance of data points around the analytic function. Then we generated a data set by drawing a noise with zero mean and that variance, and added it to the analytical function. Finally, we fitted again the parameters, with the already determined period and degree of freedom to this pseudo-data set. We repeated this procedure 1000 times, and studied the variation of the parameters. Both methods gave error estimates for the parameters within a factor of 2 from each other, which shows that our initial estimates of the uncertainties of the data points were correct. The error bars in Fig. 4 correspond to the uncertainties derived analytically from the data point uncertainties.

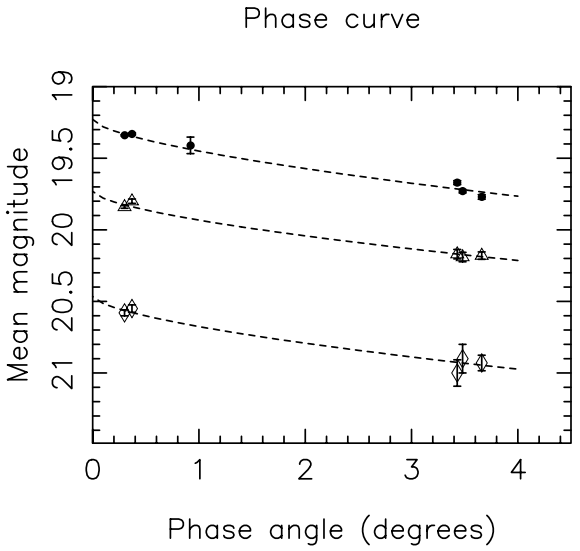

Fig. 4. Mean magnitudes (see Eq. (2)) for the *R* (filled circles), *V* (triangles) and *B* (diamonds) filters obtained with the single-peaked lightcurve. The phase curves are compared to their $H - G$ scattering parametrization.

4. Discussion

The rotational lightcurves in the three different bands present large amplitudes which appear the same within our uncertainties. Table 6 presents the peak-to-peak amplitudes computed for each of the three bands. It can be seen that the amplitude in the *B* band is slightly larger than in the *V* and *R* bands. This difference, however, is not really secure, because of the large

Table 6. Lightcurve peak-to-peak amplitudes.

	B	*V*	*R*
single-peaked lightcurve	0.60 ± 0.09	0.49 ± 0.05	0.51 ± 0.03
double-peaked lightcurve	0.76 ± 0.10	0.57 ± 0.05	0.53 ± 0.03

Table 7. Color indices of 1999 TD_{10}.

	0.3°–0.4°	3.4°–3.7°
$B-V$	0.74 ± 0.04	0.76 ± 0.11
$V-R$	0.48 ± 0.02	0.46 ± 0.04

errorbars for the *B* data. If this difference is real, nevertheless, it would imply that the light variations are mainly due to some changes in the apparent albedo when the object rotates. This cause of light variations would be confirmed by the quasi symmetry between the two parts of the rotational lightcurve when we assume it double-peaked.

On the other hand if we assume that the brightness changes are due to elongated shape it is possible to compute a lower limit for the axis ratio a/b, where a and b are the semiaxes such as $a \geq b$ (the rotation axis being supposed perpendicular to the line of sight). If Δm_R is the lightcurve amplitude we have:

$$a/b \geq 10^{0.4\Delta m_R}. \quad (3)$$

Using $\Delta m_R = 0.526$ we obtain $a/b \geq 1.62 : 1$.

The absolute magnitude *H* (see below) can also be used to derive an average radius of 1999 TD_{10}. The apparent magnitude of a KBO can be represented as:

$$m_R = m_\odot - 2.5 \log \left[\frac{p_R r^2 \phi(\alpha)}{2.25 \times 10^{16} R^2 \Delta^2} \right]. \quad (4)$$

In this formula $m_\odot$ is the apparent red magnitude of the sun (−27.1), p_R the red geometric albedo, r the radius of the object (expressed in km), $\phi(\alpha)$ is the phase function (equal to 1 for $\alpha = 0$) and R and Δ are the heliocentric and geocentric distances (expressed in AU). For $m_R = H_R$, $\phi(\alpha) = 1$ and $\Delta = R = 1$ and we obtain:

$$r = \frac{570}{\sqrt{p_v}} 10^{-0.2 H_R}. \quad (5)$$

Assuming $p_v = 0.04$ this formula leads to a diameter equal to about 120 km for 1999 TD_{10}, with $H_R = 8.37$.

From the mean magnitudes, we computed the color indices $B-V$ and $V-R$ which are given in Table 7. Since the models of physical surface properties assume that the phase effect is phase angle dependent, we computed the color indices at 2 different phase angles: in the 0.3°–0.4° and in the 3.4°–3.7° ranges. Within the precision of our data, there is no evidence of variation of color indices with the phase angle. The color indices are in good agreement with the ones published by Delsanti et al. (2001) ($V-R = 0.51 \pm 0.03$ for $\phi = 3.7°$), and by Consolmagno et al. (2000) ($B-V = 0.77 \pm 0.02$ and $V-R = 0.47 \pm 0.01$ for $\phi = 2.07°$).

The phase function reveals a significant increase of the brightness for the three bands: about 0.3 mag when phase angle α varies from 3.66 to 0.30°. Unfortunately, because of the irregular sampling of the phase angle range covered, it is impossible to know if this brightness change is linear or not in the *V* and *B* bands. For the *R* band the situation is a little bit improved by the presence of a the data obtained on October 1, at $\alpha = 0.92°$. Unfortunately this point on the phase function curve is based only on three measurements of the magnitude (see Table 3) and has, consequently, a large errorbar. Moreover its position in the phase function curve is very sensitive to the determination of the rotation period.

Table 8. H-G scattering parametrization obtained from the phase curve.

	B	*V*	*R*
H	9.61 ± 0.69	8.87 ± 0.30	8.37 ± 0.14
G	−0.14 ± 0.29	−0.09 ± 0.13	−0.19 ± 0.06

With the best estimate of the rotation period it can be seen that the phase function appears linear for the *R* band data. This linear characteristic prevents to model this phase function with any formula describing an opposition effect (see e.g. Hapke 1986; Piironeen et al. 2000 or Shevchenko 1996, 1997). In order to try to compare this phase function with the works already published we used the standard formalism of Bowell et al. (1989) with the *H* and *G* factors. Table 8 presents the results of the calculations. The absolute magnitude *H* can be used to estimate the size of the object, as explained above. The *G* factor, which is correlated to the slope of the curve, can be compared with the values obtained by other authors.

Sheppard & Jewitt (2002) presents in their Table 12 the *H* and *G* factors for seven different KBOs, observed by them at small phase angles (this phase angle is always less than 2 degrees). For all these objects $-0.44 \leq G \leq -0.04$. Bauer et al. (2002) presents some observational results obtained on Centaur 1999 UG_5, with $1 \leq \alpha \leq 7°$. The *G* factor computed from their data is −0.13. These values are consistent with our own result ($G = -0.19$ for the *R* band data).

In the Bowell formalism, negative values of *G* are not formally excluded, nevertheless it was originally designed to describe all type of surfaces with $0 \leq G \leq 1$. Since all the values given above are negative this formalism does not seem to be appropriate to describe KBOs surface, at least when a limited range of phase angle is available. It was already pointed out that this formalism fails to accurately fit the phase function for both high and low albedo asteroids (Harris et al. 1989b; Shevchenko et al. 1997). The negative G values obtained for Kuiper Belt Objects would confirm this poor capability of this formalism to describe the phase function for low albedo surfaces, since the albedo of these objects is usually assumed to be very small, compared to asteroids.

From our data, if we assume that the phase function is linear we can fit it by: $m_R = m_0 + \beta\alpha$ with $\beta = 0.121 \pm 0.003$ mag deg^{-1}. The value of β has a very poor physical meaning, since we know that the phase function is *not* linear. For the small values of α available it is even highly probable that we are already in the opposition surge and a better sampling of the phase function would probably reveals a discrepancy from the linearity. Nevertheless this parameter can help to compare with the results published by Shaefer & Rabinowitz (2002) and Sheppard & Jewitt (2002). The first authors computed a value of 0.125 mag deg^{-1} for 2000 EB_{173} observed with $0.28 \leq \alpha \leq 1.96°$ and the second have an average value of 0.15 mag deg^{-1} for the seven objects studied. Our result is on the same order of magnitude to the one already published. The relatively high value of the β parameter seems to confirm that our observations are obtained for such phase angles that the effect of the opposition surge are already apparents. Nevertheless, seen the poor sampling of our observations with respect of the phase angle variations, it cannot be excluded that more data would reveal a significant deviation from linearity and, hence, a part of the opposition surge.

5. Conclusions

The photometric data obtained with 1999 TD_{10} for different phase angles lead to the following conclusions:

(i) The rotational period is 7h41.5±0.1min if the lightcurve is single-peaked, but the data collected do not permit to distinguish between a single-peaked lightcurve or a double-peaked one.

(ii) The amplitude of the lightcurve seems to be slightly more important in the *B* band than in the *V* and *R* bands (0.60 mag and 0.51/0.49 mag), nevertheless this discrepancy is not secure, because of the large errorbar in the *B* band. If this discrepancy is real the light variations would be due mainly to albedo variations during the rotation.

(iii) No change of the color indices vs. phase angle are apparent.

(iv) The phase function seems to present a linear increase of the brightness whith decreasing phase angle. The total decrease of magnitude, when α decreases from 3.66 to 0.3° is about 0.3 mag. When assuming a linear increase of the brightness we have 0.121 ± 0.003 mag deg^{-1}.

More photometric measurements are needed to confirm the above-mentioned results. We plan to get new observations of 1999 TD_{10} and other KBOs over the next years.

References

Barucci, M. A., Romon, J., Doressoudiram, A., & Tholen, D. J. 2000, A. J., 120, 496

Bauer, J. M., Meech, K. J., Fernández, Y. R., Farnham, T. L., & Roush, T. L. 2002, PASP, 114, 1309

Belskaya, I. N., & Shevchenko, V. G. 2000, Icarus, 147, 94

Bowell, E., Hapke, B., Domingue, D., et al. 1989, in Asteroids II, ed. R. P. Binzel, T. Gehrels, & M. S. Matthews (Tucson: Univ. of Arizona Press), 524

Brown, M. E. 2000, American Astronomical Society, DPS meeting

Brown, M. E., Blake, G. A., & Kessler, J. E. 2000, ApJ 543, L163

Choi, Y. J., Prialnik, D., & Brosch, N. 2002, Asteroids, Comets, Meteor meeting, Berlin, 29 July–2 August 2002

Consolmagno, G. J., Tegler, S. C., Rettig, T., & Romanishin, W. 2000, American Astronomical Society, DPS meeting

Davies, J. K., Green, S., McBride, N., et al. 2000, Icarus, 146, 253

Delsanti, A. C., Boehnhardt, H., Barrera, L., et al. 2001, A&A, 380, 347

Drossart, P. 1993, Planet. Space Sci., 41(5), 381

Gladman, B., Kavelaars, J. J., Petit, J.-M., et al. 2001, AJ, 122, 1051

Hainaut, O. R., & Delsanti, A. C. 2002, A&A, 389, 641

Hapke, B. 1986, Icarus, 67, 264

Hapke, B., Nelson, R., & Smythe, W. 1998, Icarus, 133, 89

Harris, A. W, Young, J. W., Bowell, E., et al. 1989, Icarus, 77, 171

Harris, A. W., Young, J. W., Contreiras, L., et al. 1989b, Icarus, 81, 365

Helfenstein, P., Veverka, J., & Hillier, J. 1997, Icarus, 128, 2

Helfenstein, P., Currier, N., Clark, B. E., et al. 1998, Icarus, 135, 41

Jewitt, D. C., & Luu, J. X. 1998, AJ 15, 1667

Jewitt, D. C., & Luu, J. X. 2001, AJ 122, 2099

Lederer, S. M., Jarvis K. S., & Vilas, F. 2002, Asteroids, Comets, Meteor meeting, Berlin, 29 July–2 August 2002

McBride, N., Davies, J. K., Green, S .F., & Foster, M. J. 1999, MNRAS, 306, 799

Nelson, R. M., Hapke, B. W., Smythe, W. D., & Spilker L. J. 2000, Icarus, 147, 545

Ortiz, J. L., & Gutiérrez, P. J. 2002, Asteroids, Comets, Meteor meeting, Berlin, 29 July–2 August 2002

Ortiz, J. L., Gutiérrez, P. J., Casanova, V., & Sota, A. 2003, A&A, 407, 1149

Poulet, F., Cuzzi, J. N., French, R. G., & Dones, L. 2002, Icarus, 158, 224

Piironeen, J., Muinonen, K., Keranen, S., Karttunen, H., & Peltoniemi, J. 2000, in Observing land from space: science, customers and technology, ed. M. M. Verstraete, M. Menenti, & J. Peltoniemi (Kluwer Academics Publishers), 219

Press, W. H., Teukolsky, S. A., Vetterling, W. F., & Flannery, B. P. 1992, Numerical recipes in Fortran; the art of scientific computing, ed. W. H. Press, 2nd edn. (Cambridge University Press)

Schaefer, B. E., & Rabinowitz, D. L. 2002, Icarus, 160, 52

Sheppard, S. S., & Jewitt, D. C. 2002, AJ, 124, 1757

Shevchenko, V. G., Chiorni, V. G., Kalashnikov, A. V., et al. 1996, ApJSS, 115, 1

Shevchenko, V. G., Krugly, Yu. N., Lupishko, D. F., Harris, A. W., & Chernova, G. P. 1993, Astron. Vestn., 27, 75

Shkuratov, Y. G., & Helfenstein, P. 2001, Icarus, 152, 96

Trujillo, C. A., Jewitt, D. C., & Luu, J. X. 2001, AJ 122, 457

Trujillo, C. A., & Brown, M. E. 2002, ApJ, 566, L125